

addition to the ring charges, two sets of point charges are positioned on the Z-axis as shown in Fig. 1. Each set has two point charges one inside the particle and the other outside the particle. Thus, the total number of unknowns is $2N + 4$.

To determine the values of the unknown charges q_j , $j = 1, 2, \dots, 2N + 4$, N boundary points are selected around the particle surface. The boundary points have the same Z-coordinates as those of the simulation ring charges, Fig. 1. This is in addition to two boundary points on the Z-axis as shown in Fig. 1. Thus, the total number of boundary points is $N + 2$.

At each boundary point, two boundary conditions are satisfied, namely; the continuity of potential (Dirichlet condition) and the continuity of the electric flux.

$$\varphi_1(r_b, z_b) = \varphi_2(r_b, z_b) \quad (1)$$

The potential $\varphi_1(r_b, z_b)$ at the point (r_b, z_b) is the algebraic sum of potentials at the point due to the charged plates and the inner simulation charges (N rings and 2 point charges) if the point is seen from the medium side. If the boundary point is seen from the particle side, the potential $\varphi_2(r_b, z_b)$ is the algebraic sum of the potentials due to the charged plates and the outer simulation charges (N rings and 2 point charges). The potential at the boundary point due to the applied field E_0 is expressed as:

$$\phi(r_b, z_b) = V_0 z_b / L \quad (2)$$

The continuity of the electric flux at a boundary point (r_b, z_b) is expressed as:

$$\varepsilon_1 E_{n1}(r_b, z_b) = \varepsilon_2 E_{n2}(r_b, z_b) \quad (3)$$

If the point is seen from the medium side, the component $E_{n1}(r_b, z_b)$ of the electric field normal to the particle surface at the point (r_b, z_b) is the vectorial sum of the normal component of the applied field E_0 and the normal field components due to the inner simulation charges, all calculated at this point.

If the boundary point is seen from the particle size, the normal component $E_{n2}(r_b, z_b)$ of the electric field is the vectorial sum of the normal field component of the applied field E_0 and the normal field components due to the outer simulation charges, all calculated at this point.

Applying the two boundary conditions, namely; the continuity of potential and electric flux, at all boundary points (of number = $2N + 2$) formulates $2N + 4$ equations into $2N + 4$ unknowns. Simultaneous solution of these equations

determines the unknown simulation charges. Once the unknown charges are determined, the electric field can be calculated inside and outside the particle. The interface charge or the polarization surface charge σ_{sp} at a point (r_b, z_b) on the particle surface is determined as equal to the change of the normal electric flux at the point when seen from the medium and the particle sides, i.e.

$$\sigma_{sp} = \varepsilon_2 E_{n2}(r_b, z_b) - \varepsilon_1 E_{n1}(r_b, z_b) \quad (4)$$

where ε_1 and ε_2 are, respectively, the permittivity of the surrounding medium and the particle.

II.2. Particle During Charging

With the flow of the space charge along the applied field, the particle is charged and the boundary conditions determining the unknown charges are different from those before particle charging. The Dirichlet boundary condition is still valid. The continuity condition of electric flux is substituted by the continuity of the current density at each boundary point.

The continuity of the current density at a boundary point (r_b, z_b) is expressed as:

$$J_{n1} = J_{n2}$$

$$\text{Hence; } \sigma_1 E_{n1}(r_b, z_b) = \sigma_2 E_{n2}(r_b, z_b) \quad (5)$$

where σ_1 and σ_2 are respectively the conductivity of the surrounding medium and the particle. J_{n1} and J_{n2} are the current density at the boundary point when seen from the medium and particle sides.

Corresponding to E_{n1} and E_{n2} , the electric-flux density values are:

$$D_{n1} = \mathbf{e}_1 E_{n1} = \mathbf{e}_1 \frac{J_{n1}}{\mathbf{s}_1}$$

$$D_{n2} = \mathbf{e}_2 E_{n2} = \mathbf{e}_2 \frac{J_{n2}}{\mathbf{s}_2} = \mathbf{e}_2 \frac{J_{n1}}{\mathbf{s}_2}$$

The surface charge density

$$\mathbf{s}_s = D_{n2} - D_{n1} = J_{n1} \left(\frac{\mathbf{e}_2}{\mathbf{s}_2} - \frac{\mathbf{e}_1}{\mathbf{s}_1} \right) = \mathbf{s}_1 E_{n1} \left(\frac{\mathbf{e}_2}{\mathbf{s}_2} - \frac{\mathbf{e}_1}{\mathbf{s}_1} \right) \quad (6)$$

The surface charge density σ_{sc} due to particle charging by corona ions is expressed as

$$\sigma_{sc} = \sigma_s - \sigma_{sp} \quad (7)$$

III. Results and Discussion

For an applied field E_0 of 1 V/m, Fig.2 shows how the electric field E_2 inside the particle decreases with the increase of the particle conductivity σ_2 for

the same conductivity value of the surrounding medium ($\sigma_1 = 10^{-9} \text{ } \Omega^{-1} \cdot \text{m}^{-1}$). The field E_2 approaches the zero value at high σ_2 values ($\sigma_2 = 10^{-7} \text{ } \Omega^{-1} \cdot \text{m}^{-1}$) where the particle behaves as a conducting sphere in a uniform field. On the other hand, the value of E_2 approaches the limiting value of 1.5 times the applied field E_0 at low σ_2 values ($\sigma_2 = 10^{-12} \text{ } \Omega^{-1} \cdot \text{m}^{-1}$). This conforms with the field values of the case of a perfect insulating sphere positioned in a uniform field.

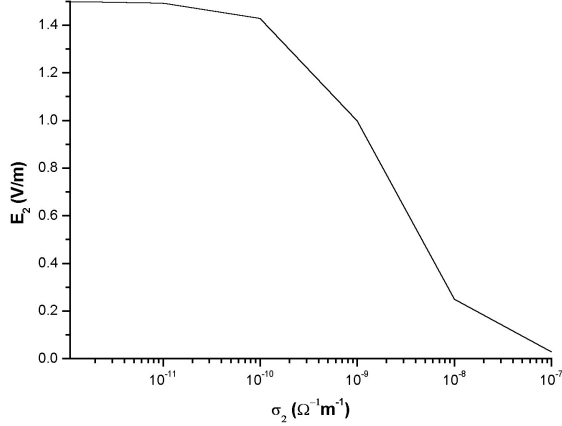


Fig. 2. Electric field E_2 inside the particle against the particle conductivity σ_2 for the same conductivity value of the surrounding medium ($\sigma_1 = 10^{-9} \text{ } \Omega^{-1} \cdot \text{m}^{-1}$, $E_0 = 1 \text{ V/m}$).

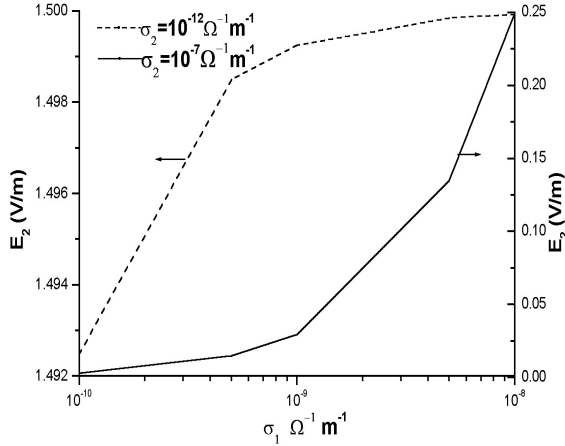


Fig. 3. Electric field E_2 inside the particle against the conductivity σ_1 of the surrounding medium for two different values of the particle conductivity σ_2 ($E_0 = 1 \text{ V/m}$)

For an applied field E_0 of 1 V/m, Fig.3 shows how the electric field E_2 inside the particle depends on the conductivity σ_1 of the surrounding medium for two different values of the particle conductivity σ_2 (10^{-12} and $10^{-7} \text{ } \Omega^{-1} \cdot \text{m}^{-1}$). As long as $\sigma_2 \ll \sigma_1$, the particle behaves as an insulating sphere and the field E_2 inside the particle approaches the limiting value $1.5 E_0$. This conforms with Fig.3 for $\sigma_2 = 10^{-12} \text{ } \Omega^{-1} \cdot \text{m}^{-1}$, where the value of E_2 increases from $1.492 E_0$ to reach the limiting value $1.5 E_0$ as the ratio σ_2/σ_1 , decreases from 10^{-2} to 10^{-4} . On the other hand, the value of E_2 approaches the zero value

when $\sigma_2 \gg \sigma_1$, where the particle behaves as a conducting sphere. This conforms with Fig.3 for $\sigma_2 = 10^{-7} \text{ } \Omega^{-1} \cdot \text{m}^{-1}$, where the value of E_2 decreases from 0.25 to about 0.01 as the ratio σ_2/σ_1 , increases from 10 to 1000.

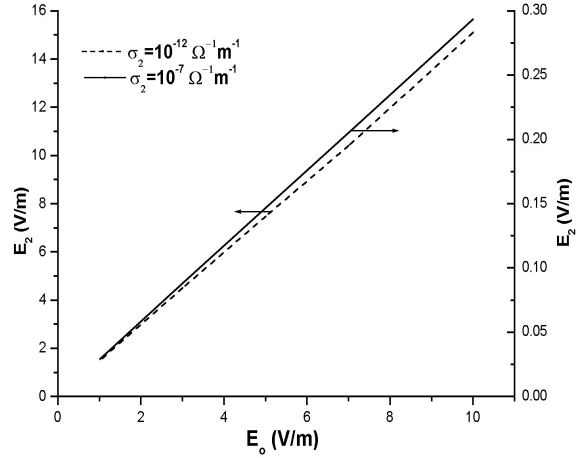


Fig. 4. Dependency of the electric field E_2 inside the particle on the applied field E_0 for two different values of the particle conductivity σ_2 ($\sigma_1 = 10^{-9} \text{ } \Omega^{-1} \cdot \text{m}^{-1}$).

For a conductivity value σ_1 of $10^{-9} \text{ } \Omega^{-1} \cdot \text{m}^{-1}$, Fig.4 shows how the electric field E_2 inside the particle depends on the applied field E_0 for two different values of the particle conductivity σ_2 (10^{-12} and $10^{-7} \text{ } \Omega^{-1} \cdot \text{m}^{-1}$). For $\sigma_2 = 10^{-12} \text{ } \Omega^{-1} \cdot \text{m}^{-1}$, the ratio σ_2/σ_1 equals 10^{-3} and the particle behaves as an insulating sphere where the field E_2 is 1.5 times E_0 . This explains the linear relationship shown in Fig.4 between E_2 and E_0 with slope equals 1.5 for $\sigma_2 = 10^{-12} \text{ } \Omega^{-1} \cdot \text{m}^{-1}$. On the other hand, the ratio σ_2/σ_1 equals 10^2 for $\sigma_2 = 10^{-7} \text{ } \Omega^{-1} \cdot \text{m}^{-1}$ and the particle behaves approximately as a conducting sphere where the field E_2 inside the particle assumes low values with respect to applied field E_0 . Therefore, the linear relationship between E_2 and E_0 for $\sigma_2 = 10^{-7} \text{ } \Omega^{-1} \cdot \text{m}^{-1}$ dictates a value of E_0 around 0.29 V/m against 10 V/m for the applied field E_0 , Fig.4.

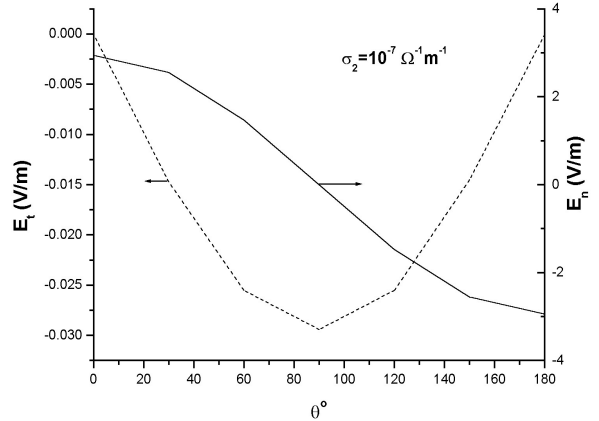


Fig. 5a. Variation of the normal E_n and tangential E_t components of the electric field over the particle surface ($0 \leq \theta \leq 180^\circ$) ($\sigma_1 = 10^{-9} \text{ } \Omega^{-1} \cdot \text{m}^{-1}$, $E_0 = 1 \text{ V/m}$).

For a conductivity value σ_1 of $10^9 \text{ } \Omega^{-1} \cdot \text{m}^{-1}$ of the surrounding medium, Fig.5a shows the variation of the normal and tangential components of the field E_1 over the surface of the particle with conductivity $\sigma_2 = 10^7 \text{ } \Omega^{-1} \cdot \text{m}^{-1}$. A conducting sphere positioned in a uniform field E_0 distorts the field which reaches a limiting value of $3 E_0$ where the field meets the sphere, Fig.1. At $\delta=0$, the normal component E_n of the surface field E_1 is equal to $3E_0$ providing that E_0 extends along the Z-axis, Fig.1. At $\delta= \delta$, $E_n = -3E_0$. Subsequently, the tangential component E_t of the surface field E_1 is zero at $\delta=0$ and $\delta= \delta$. With the decreases of δ , the normal component E_n decrease from the value $3 E_0$ reaching the zero value at $\delta= \delta/2$ and $-3E_0$ at $\delta= \delta$. This conforms with Fig.5a where the normal component E_n changes between the limits $\pm 2.9E_0$, with $E_0 = 1 \text{ V/m}$.

On the contrary, the tangential field E_t increases with the increase of δ starting from $\delta=0$ reaching its maximum value at $\delta= \delta/2$. As the particle behaves as a conducting particle, the maximum value of the tangential field is small with respect to the maximum value of the normal component. This is quite clear from the respective values of the normal and tangential field components of Fig.5a.

For a conductivity value σ_1 of $10^9 \text{ } \Omega^{-1} \cdot \text{m}^{-1}$ of the surrounding medium, Fig.5b shows the variation of the normal E_n and tangential E_t components of the field E_1 over the surface of a particle with conductivity $\sigma_2 = 10^{12} \text{ } \Omega^{-1} \cdot \text{m}^{-1}$. As $\sigma_2 \ll \sigma_1$, the particle behaves oppositely to that of the conducting sphere and the maximum value of the tangential field is significantly high with respect to the maximum value of the normal component. However, the trend of variation of the normal and tangential components of the field over the particle surface as shown in fig. 5b is the same as that for the conducting particle in Fig. 5a.

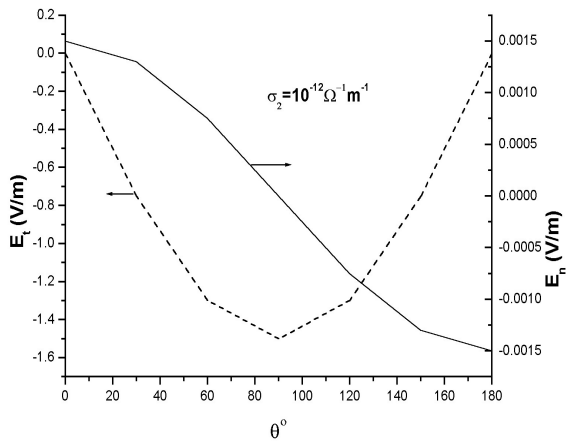


Fig. 5b. Variation of the normal E_n and tangential E_t components of the electric field over the particle surface ($0 \leq \theta \leq 180^\circ$) ($\sigma_1 = 10^9 \text{ } \Omega^{-1} \cdot \text{m}^{-1}$, $E_0 = 1 \text{ V/m}$).

For an applied field E_0 of 1 V/m and conductivity value σ_1 of $10^9 \text{ } \Omega^{-1} \cdot \text{m}^{-1}$, Fig.6 shows the distribution of the polarization charge density σ_{sp} over the particle surface for two different values of the particle conductivity σ_2 (10^{12} and $10^7 \text{ } \Omega^{-1} \cdot \text{m}^{-1}$). The surface charge density σ_{sp} depends not only on the conductivity values σ_2 and σ_1 of the particle and the surrounding medium, but also on the respective values of the permittivity $\hat{\epsilon}_2$ and $\hat{\epsilon}_1$. In Fig.6, $\hat{\epsilon}_1$ is that of the surrounding gas ($=\hat{\epsilon}_0$) and $\hat{\epsilon}_2$ of the particle permittivity is $3\hat{\epsilon}_0$, where $\hat{\epsilon}_0$ is the permittivity of free space. For $\sigma_2 = 10^7 \text{ } \Omega^{-1} \cdot \text{m}^{-1}$, the particle behaves as a conducting sphere and a surface charge appears on the particle to account for diminishing the field inside. The surface charge is of negative sign on the incident part of the sphere and of positive sign on the backward part. The surface charge density σ_{sp} changes from maximum positive at $\delta=0$ to maximum negative at $\delta= \delta$. The charge density σ_{sp} takes zero value at $\delta= \pm\delta/2$ as shown in Fig.6. It is worthy to mention that total charge on the entire particle is zero.

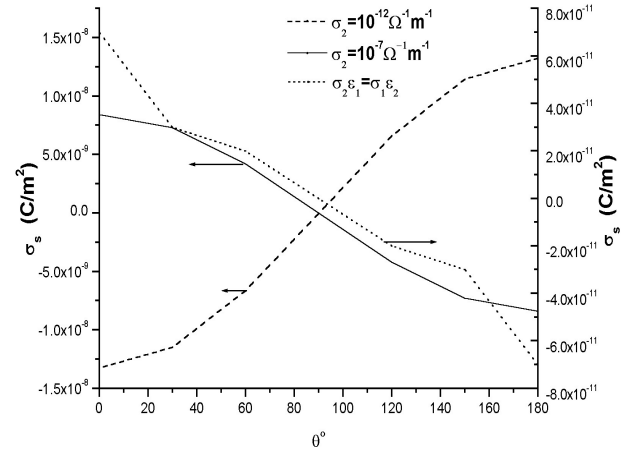


Fig. 6. Variation of the interfacial surface charge density σ_s over the particle surface ($0 \leq \theta \leq 180^\circ$) for two different values of the particle conductivity σ_2 and for the condition $\sigma_2 \epsilon_1 = \sigma_1 \epsilon_2$ ($\sigma_1 = 10^9 \text{ } \Omega^{-1} \cdot \text{m}^{-1}$, $E_0 = 1 \text{ V/m}$).

For $\sigma_2 = 10^{12} \text{ } \Omega^{-1} \cdot \text{m}^{-1}$, the particle behaves as an insulating sphere and an interfacial surface charge appears to conduct the electric field E_2 inside the particle. The interfacial charge is of positive sign on the incident part of the sphere and of negative sign the backward part. The interfacial charge density changes from maximum negative at $\delta=0$ to maximum positive at $\delta= \delta$ with a zero value at $\delta= \pm\delta/2$ as shown in Fig.6. Also, the total charge on the entire particle is zero, the same as the case of a conducting particle of $\sigma_2 = 10^7 \text{ } \Omega^{-1} \cdot \text{m}^{-1}$. Fig.6 shows also the surface charge density σ_{sp} over the sphere for the condition $\epsilon_1 \sigma_2 = \epsilon_2 \sigma_1$ ($\epsilon_1 = \epsilon_0$ and $\epsilon_2 = 100\epsilon_0$; $\sigma_1 = 10^9 \text{ } \Omega^{-1} \cdot \text{m}^{-1}$ and $\sigma_2 = 10^7 \text{ } \Omega^{-1} \cdot \text{m}^{-1}$), which is negligible in comparison with the discussed case of

$\sigma_2 = 10^{-7} \hat{U}^{-1} \cdot m^{-1}$. This condition corresponds to equality of the relaxation time in both the particle and the surrounding medium, where there is no chance for surface charge to appear in conformity with the charge density values reported in Fig.6 for the case of $\sigma_2 = 10^{-7} \hat{U}^{-1} \cdot m^{-1}$. Theoretically speaking, the charge density at the condition $\epsilon_1 \sigma_2 = \epsilon_2 \sigma_1$ is zero as depicted by eqn. (6).

The positive ion flow of density \tilde{n} ($6.6 \times 10^{-6} C/m^3$) takes place along the field lines that start far away (at $Z = -L/2$, Fig.1) and approach the particle to charge it where the radial electric field is negative. The charge density over the particle surface is expressed by eqn.(6). For an interfacial charge to appear on the particle surface under the conditions: $\epsilon_1 = \epsilon_0$, $\sigma_1 = 10^{-9} \hat{U}^{-1} \cdot m^{-1}$, $\sigma_2 = 10^{-7} \hat{U}^{-1} \cdot m^{-1}$, the permittivity ϵ_2 of the particle should exceed $100\epsilon_0$. The charge density σ_{sc} due to corona ion charging calculated according to eqn. (7) vary around the particle as shown in Fig.7 for $\epsilon_2 = 1000\epsilon_1$ and two different values of the applied field E_0 . It is quite clear that the charge density σ_{sc} is almost constant around the particle and increases linearly with the value of the applied field. The almost uniform distribution of the charge (σ_{sc} is almost constant) over the particle surface, Fig 7, is explained by the fact that the particle behaves as a conducting sphere. This is because the particle conductivity σ_2 is much larger than σ_1 of the surrounding medium and the particle permittivity is 1000 times ϵ_0 of the surrounding medium. Therefore, the charge received by the particle from the ions distributes itself uniformly on the surface and increases with the applied field up to the saturation value Q_{max} calculated by Pauthenier and Moreau-Hanot classical formula [5]:

$$Q_{max} = 12 \delta \epsilon_1 E_0 R^2 \quad (8)$$

where R is the particle radius.

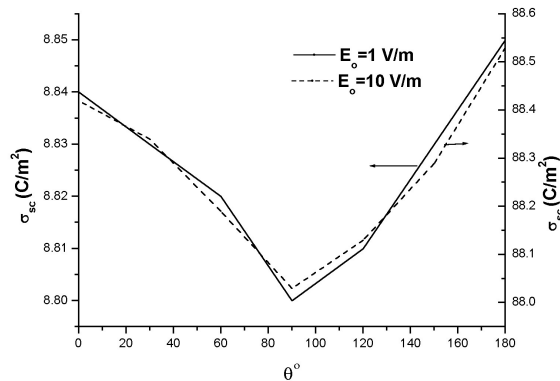


Fig. 7 Variation of the charge density σ_{sc} due to corona charging over the particle surface ($0 \leq \theta \leq 180^\circ$) for two different values of the applied field E_0 . ($\sigma_1 = 10^{-9} \hat{U}^{-1} \cdot m^{-1}$, $\sigma_2 = 10^{-7} \hat{U}^{-1} \cdot m^{-1}$, $\epsilon_1 = \epsilon_0$ and $\epsilon_2 = 1000 \epsilon_0$)

IV. Conclusions

On the basis of the present analysis, one may draw the following conclusions for spherical particles:

- (1) In absence of corona ions, the conductivity value of the particle determines how high is the electric field inside the particle. For perfect insulating particles, the inside field reaches the limit of about 1.5 times the applied dc field. On the other hand, the inside field diminishes down to zero for conducting particles.
- (2) In absence of corona ions, the conductivity value σ_1 of the surrounding medium also determines the field inside the particle. For $\sigma_2 \gg \sigma_1$, the particle behaves as a conducting sphere. On the other hand, the particle behaves as an insulating sphere for $\sigma_2 \ll \sigma_1$.
- (3) In absence of corona ions, the field inside the particle is directly related to the applied dc field irrespective of the value of the particle conductivity.
- (4) In absence of corona ions, the normal component of the field over the surface of a conducting particle is dominating with respect to the tangential component. On the contrary, the tangential component for an insulating particle is dominating with respect to the normal component.
- (5) With particle charging by corona ions, the charge density distribution over the particle surface is almost uniform for conducting particles. The value of the charge density increases linearly with the value of the applied dc field.

V. References

- [1] M. Abdel-Salam, Applications of High Voltages Engineering in Industry in "High Voltage Engineering-Theory and Practice", eds. M. Abdel-Salam et. al., Marcel Dekker, Inc., New York, USA, August 2000.
- [2] H. Singer et. al., "A charge simulation method for the calculation of high voltage fields", IEEE Trans., Vol. PAS 93, pp. 1660 – 1668, 1974.
- [3] K. Adamiak, "Rate of charging of spherical particles in mono-ionized electric fields", Proc. IEEE-IAS Annual Meeting, Chicago, USA, PP. 404-411, Sept./Oct. 2001.
- [4] L. Dascalescu et. al., "Changing of one or several cylindrical particles in mono ionized electric fields", Porch. IEEE-IAS Annual Meeting Chicago, USA, pp. 404-411, Sept./Oct. 2001
- [5] M. M. Pauthenier and M. Moreau-Hanot, "La charge des particules spheriques dans un champ ionis", Journal de Physique at le Radium, Vol.3, pp.59-61, 1932.

